Supporting Information

Nickel-Gallium-Catalyzed Electrochemical Reduction of CO_2 to Highly Reduced Products at Low Overpotentials

Daniel A. Torelli[¶†‡], Sonja A. Francis[¶†‡£], J. Chance Crompton[†‡], Alnald Javier[‡], Jonathan R. Thompson[I], Bruce S. Brunschwig*[§], Manuel P. Soriaga*[‡], and Nathan S. Lewis*[†‡§]

[†]Division of Chemistry and Chemical Engineering, [‡]Joint Center for Artificial Photosynthesis, [£]Resnick Sustainability Institute, [I]Division of Engineering and Applied Sciences, and [§]Beckman Institute Molecular Materials Research Center, California Institute of Technology, Pasadena, California 91125, United States

¶These authors contributed equally to this work

*E-mail: bsb@caltech.edu, msoriaga@caltech.edu, nslewis@caltech.edu

Experimental.

Sample Preparation.

Quartz slides (VWR), gallium (III) nitrate hydrate 99.999% [69% gallium by mass] (Sigma Aldrich) and nickel (II) nitrate hexahydrate 99.999% (Sigma Aldrich) were used as received. Pyrolytic graphite plates (GraphiteStore) were cleaned in aqua regia and polished to a mirror finish before use. Water with a resistivity > 18 MΩ cm obtained from a Barnsted Nanopure system was used throughout.

Aqueous stock solutions of 0.052 M nickel nitrate and 0.036 M gallium nitrate were prepared and were combined in appropriate ratios to prepare precursor solutions for NiGa, Ni_5Ga_3, and Ni_3Ga. For an individual sample, 0.5 mL of the precursor solution was drop-cast onto a graphite plate heated to 100 °C. After drying on a hotplate for five min, the samples were placed in porcelain boats and then loaded into a quartz tube in a Carbolite tube furnace. The tube furnace was placed under a constant 4 L min^{-1} flow of forming gas (5% H_2, 95% N_2) and then heated to 700 °C for 3 h, before cooling to room temperature. The back of the graphite plate was then covered in 3M 470 Electroplating Tape (Uline.com) to mask from electrical contact with the solution, and an alligator clip was used to make contact to the front part of the plate with the Ni_xGa_y film. Control Ni-only samples and Ga-only samples were made by the same method but only drop-casting one of the precursor solutions.

Powder X-ray diffraction (XRD) patterns were collected at room temperature on a Bruker D2 Phaser Diffractometer with a copper Kα source (λ = 1.54184 Å) and a LynxEye-1D detector. Simulated XRD patterns were generated by the Crystal Maker and Crystal Diffract software package.

Electrochemical Testing.

A BioLogic SP-200 potentiostat (Biologic, Grenoble, France) was used for all electrochemical testing. The uncompensated cell resistance was determined from a single-point high-frequency impedance measurement and was compensated (85%) by the built-in positive-feedback software. A modified two-compartment cell was used for all electrochemical measurements. The cell consisted of a Pyrex weigh bottle that had been modified with ground-glass joints in its lid (Figure S3). The joints were used to insert electrodes and make seals during electrolysis, while the bottle was used so that the entire lid of the cell could be removed to accommodate larger (2-4 cm^2) working electrodes. A polyether ether ketone (PEEK) tube was modified with a detachable ring at the bottom that was fit with a fresh Selemion anion-exchange membrane before each electrolysis or set of cyclic voltammograms (CV). The Pt mesh counter electrode was behind the membrane. A Ag/AgCl (3M NaCl) fritted reference electrode (CH Instruments) was used, and potentials were converted to values relative to a reversible hydrogen electrode (RHE) using the equation: E (vs. RHE) = E (vs. Ag/AgCl) + 0.197 V + 0.0591 V x pH. The working electrode was the Ni-Ga film supported on the graphite plate described above. Electrical contact was made with a stainless steel alligator clip. The electrolyte used in all cycling tests was potassium phosphate buffered to pH 7. No anodic cycling was performed before electrolyses. All cycling was performed on fresh electrodes to show their electrochemical behavior. During the first minute of electrolysis, the current decreased by ~5-10x as the native oxide was reduced. At these

potentials, a Pourbaix diagram shows that only the metallic state of Ni is stable. Bulk electrolysis was performed in a cell that was sealed under 1 atm CO_2 and stirred at ~ 1,000 rpm. Electrolyses were performed at varied potentials ranging from -0.9 V to -1.8 V versus a Ag/AgCl (3 M NaCl) reference electrode, in 0.1 M Na_2CO_3 (Sigma-Aldrich ≥ 99.999% metal basis) that had been acidified to pH 6.8 with 1 atm CO_2 creating a HCO_3^-/CO_2 buffered system similar to the standard protocol.[1] Na_2CO_3 was used instead of $KHCO_3$ due to the much higher purity available for Na_2CO_3. Although the faradaic efficiency can be affected by the cation in the electrolyte, for a Cu electrode, the production of C_2 products is lower for Na^+ than K^+.[3] It is consequently reasonable to assume similar, if not higher, yields of C_2 products with Ni_xGa_y when a $KHCO_3$ electrolyte is used instead of $NaHCO_3$. Electrolyses were performed until a set amount of charge, generally 40 C cm^{-2} was passed. However, for some of the lower potentials, a lower amount of charge was passed in the experiments. Electrolyses at -0.5 V were run for >12 h to obtain a significant concentration of the products. The calculated yields suggest the electrodes are stable on this timescale. In contrast, polycrystalline Cu has been reported to deactivate over the same period of time, at the same potential.[6] Additionally, the $^{13}CO_2$ experiment was run for > 10 h with a data point approximately every 2 h. No decreases in the rates of $^{13}CH_4$, $^{13}C_2H_4$, or $^{13}C_2H_6$ were observed over this period of time.

CO Reduction.

For experiments where CO or N_2 was required, K_2HPO_4 was used as the electrolyte and buffered to pH 7 to create similar conditions to those under CO_2. The use of the CO_2-free buffer eliminates the possibility that CO_2 produced from the equilibration of HCO_3^- with CO_2 was responsible for the measured response rather than being attributable to CO or N_2. The CV data suggest that Ga slows the binding of CO rather than weakens the Ni-CO interaction. The potential at which CO oxidation is observed does not shift significantly (<50 mV) between the Ni film and the Ni_5Ga_3 film, suggesting that the strength of the metal-CO bond is approximately equivalent between the two films. However, the time it takes for CO to rebind is significantly longer on the Ni_5Ga_3 film compared to the Ni film, suggesting the presence of kinetic differences between the two films. Direct infrared spectroscopic detection of surface-bound CO on the Ni-Ga systems has not been observed to date.

Product Analysis.

An Agilent 7890A gas chromatograph (GC), with two thermal conductivity detectors, was used to separate and quantify the gases in the headspace of the electrochemical cell. The oven was set to 50 °C for 9 min followed by ramping at a rate of 8 °C min^{-1} to 80 °C for a total run time of 14 min. For isotopic labeling experiments that involved smaller amounts of charge passed, an Agilent 7820A GC coupled with a 5977E MS with a heated cold quadrupole detector and a capillary CarbonPLOT column was used for identification and quantification of the products. The oven was set to 35 °C for 6.6 min and was then ramped to 150 °C at a rate of 20 °C min^{-1} and held for 2 min to allow heavier molecules such as ethylene and ethane to elute. Both the GC and GCMS instrumentation was calibrated using tanks of 15% CH_4, 10% C_2H_4, and 5% C_2H_6 each mixed with N_2. Dilutions were performed by filling a sealed 1 or 3 L round-bottom flask with N_2 or CO_2, and injecting known amounts of the calibration gas. The gaseous mixture was allowed to stir for ~1 min at which time aliquots were removed for GC or GCMS calibration. ^1H NMR spectroscopy was performed on a Bruker 400 MHz Spectrometer. Standards of 10 to 100 μM solutions of the analytes (sodium formate, methanol, etc.) were prepared by serial dilution,

and were used to calibrate the instrument. In general, 0.1 μL of the internal standard (dimethyl formamide, DMF) was added to a 2 mL aliquot of the standard solution. 0.5 mL of this solution was then transferred to a NMR tube that contained 200 μL of deuterated water. A water suppression method was used to suppress the signal of the water in the electrolyte and to allow visualization of the analyte peaks. The same procedure was used to quantify the liquid CO_2 reduction products, with 0.1 μL of DMF added to 2 mL of the electrolyte after electrolysis, and 0.5 mL of this solution added in an NMR tube to 200 μL of D_2O.

Surface Analysis.

Scanning-electron micrographs were obtained using a Nova NanoSEM 450 microscope (FEI, Hillsboro, OR, USA) with an accelerating voltage of 20 kV and a working distance of 5.0 mm. X-ray photoelectron spectroscopy (XPS) data were obtained using an AXIS Ultra DLD instrument (Kratos Analytical) at a background pressure of 1×10^{-9} Torr. High-intensity excitation was provided by monochromatic Al Kα X-rays having an energy of 1486.6 eV with an instrumental resolution of 0.2 eV full width at half-maximum. Photoelectrons were collected at 0° from the surface normal at a retarding (pass) energy of 80 eV for the survey scans, whereas a pass energy of 20 eV was used for the high-resolution scans. The peak energies were calibrated against the binding energy, BE, of the adventitious C 1s peak. For quantitative analysis, the XPS signals were fitted using CasaXPS software (CASA Ltd., Teignmouth, United Kingdom) to symmetric Voigt line shapes that were composed of Gaussian (70%) and Lorentzian (30%) functions that employed a Shirley background. Electrochemical surface area measurements were preformed and electrodes were found to be only slightly roughened.

Tables and Figures.

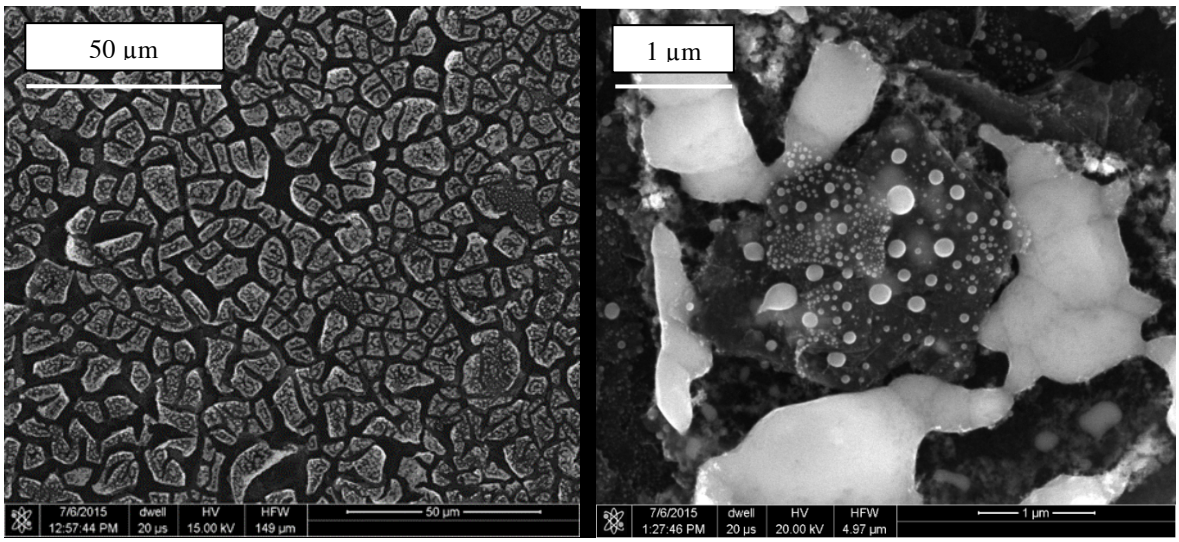

Figure S1. SEM of Ni_xGa_y films after annealing showing the aggregation of microparticles into a cracked film, (right) zoomed out, (left) zoomed in.

Table S1. Tabulated XRD reflections seen for each nickel-gallium phase.

NiGa		Ni_5Ga_3		Ni_3Ga	
2 Theta	Reflection	2 Theta	Reflection	2 Theta	Reflection
44.4	110	43.2	221	43.5	111
64.6	200	48.4	131	50.9	200
76.7	quartz	50.9	220 (Ni_3Ga)	74.8	220
81.7	211	54.5	440	76.7	quartz
94.1	quartz	75.2	440	90.8	311
98	220	76.7	quartz	94.1	quartz
		86.5	223	96.1	222
		94.1	quartz		

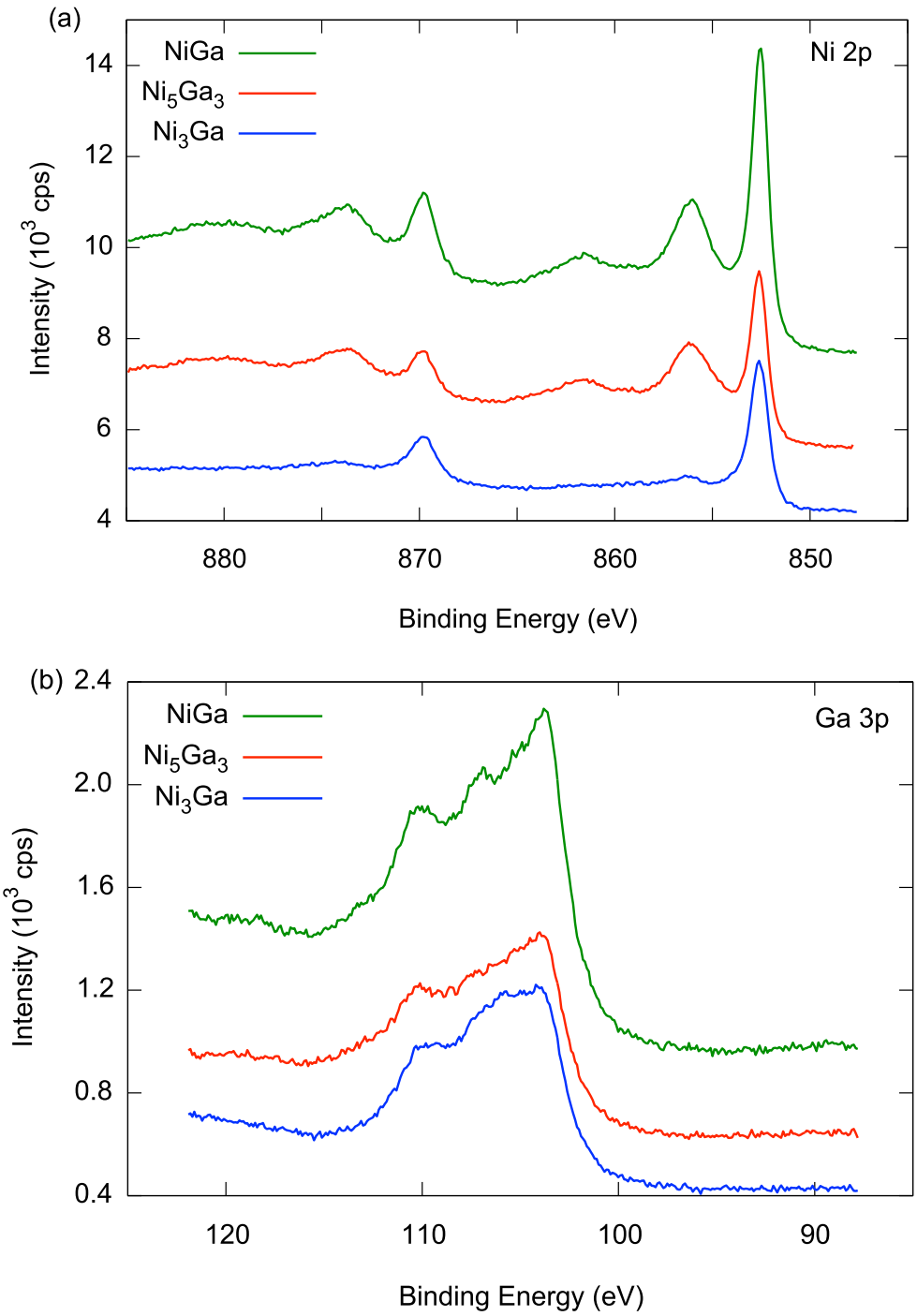

Figure S2. XP spectra showing (a) the Ni 2*p* and (b) Ga 3*p* regions. In the Ni spectra the peaks at ~852 eV and ~870 eV correspond to Ni in the nickel-gallium films, while the peaks at ~856 eV and ~874 eV correspond to oxidized Ni. Other peaks in the Ni spectra are satellite peaks. In the Ga 3p region the peaks at ~106 eV and ~109 eV correspond to oxidized Ga while the small peak at ~104 eV corresponds to metallic Ga.

Table S2. Comparison of the stoichiometric ratios of Ga 2*p* and Ni 2p from XPS data to the target values.

Phase	Ga 2*p*	Ni 2*p*	Observed Ni:Ga	Target Ni:Ga
NiGa	51	49	0.95	1
Ni_3Ga	28	72	2.53	3
Ni_5Ga_3	43	57	1.35	1.667

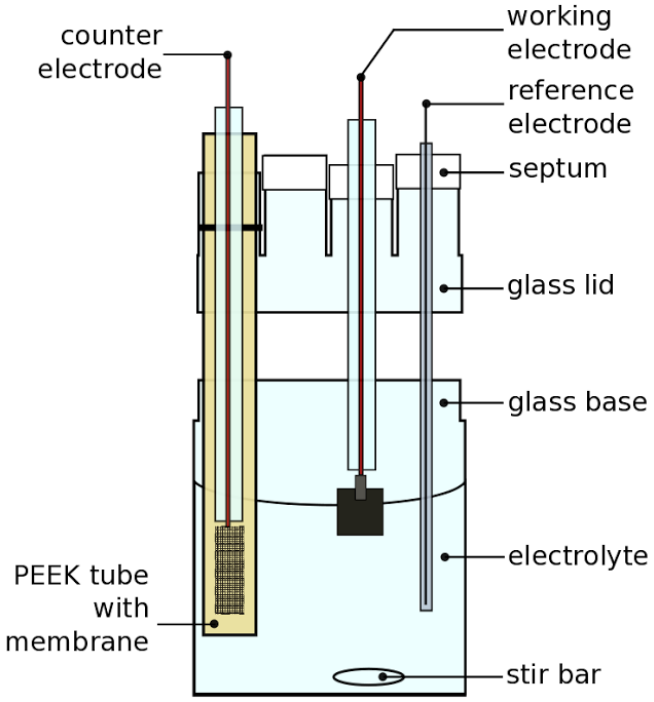

Figure S3. Diagram of the cell design employed in this study.

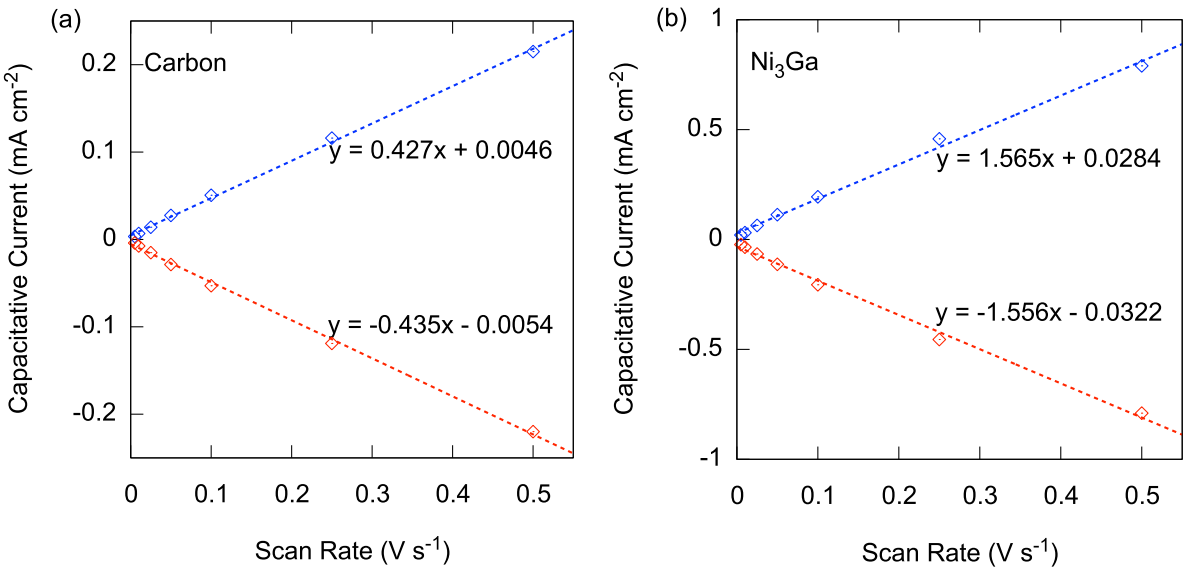

Figure S4. Electrochemical surface area measurements showing a slightly roughened film by lower (a) capacitative current on carbon substrate compared to (b) capacitative current on Ni_3Ga.

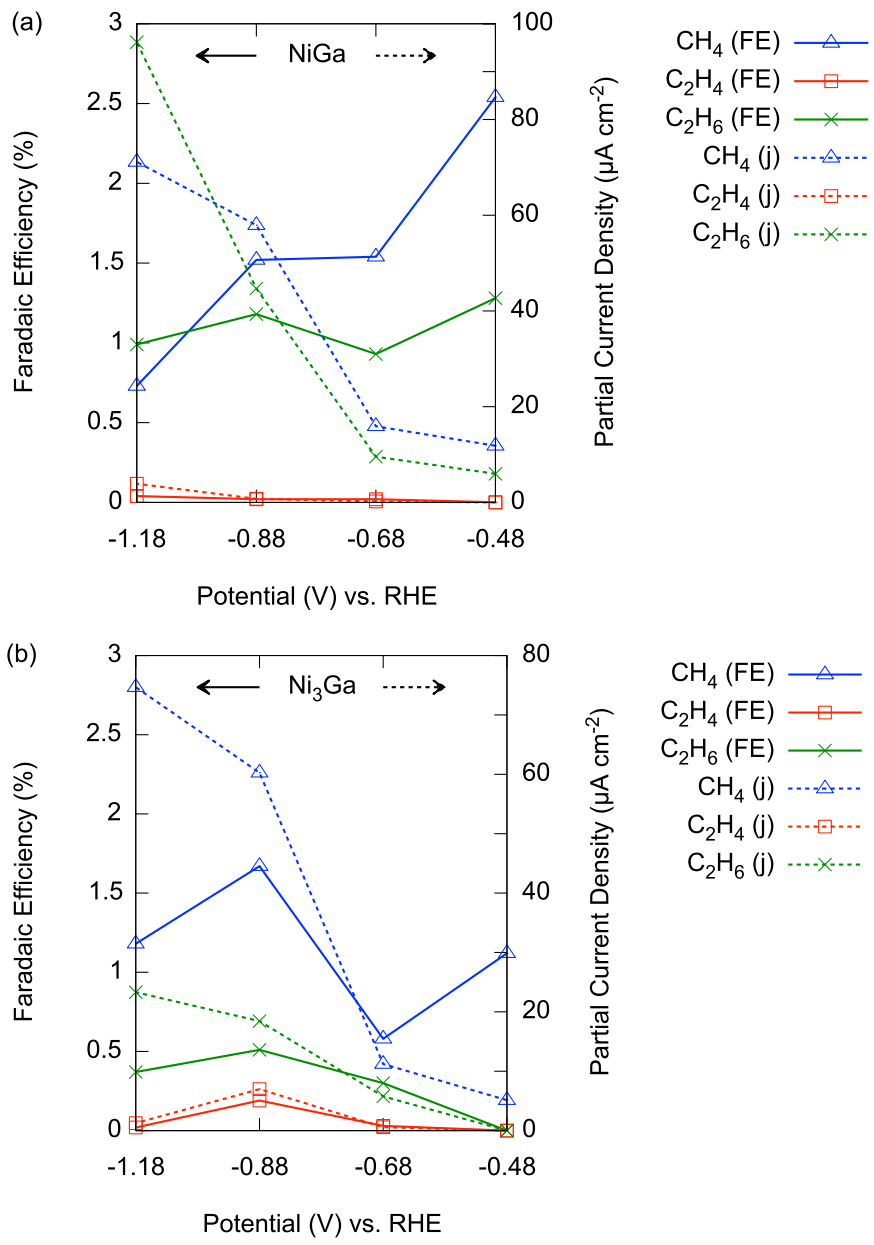

Figure S5. Potential-dependent Faradaic efficiencies (solid lines) and current densities (dotted lines) for CO_2 reduction in 0.1M Na_2CO_3 (aq) acidified to pH 6.8 with 1 atm CO_2 (g) to methane (triangles), ethylene (squares) and ethane (exes). (a) NiGa and (b) Ni_3Ga show similar behavior to Ni_5Ga_3 (See Figure 2a) with respect to product distributions at different potentials.

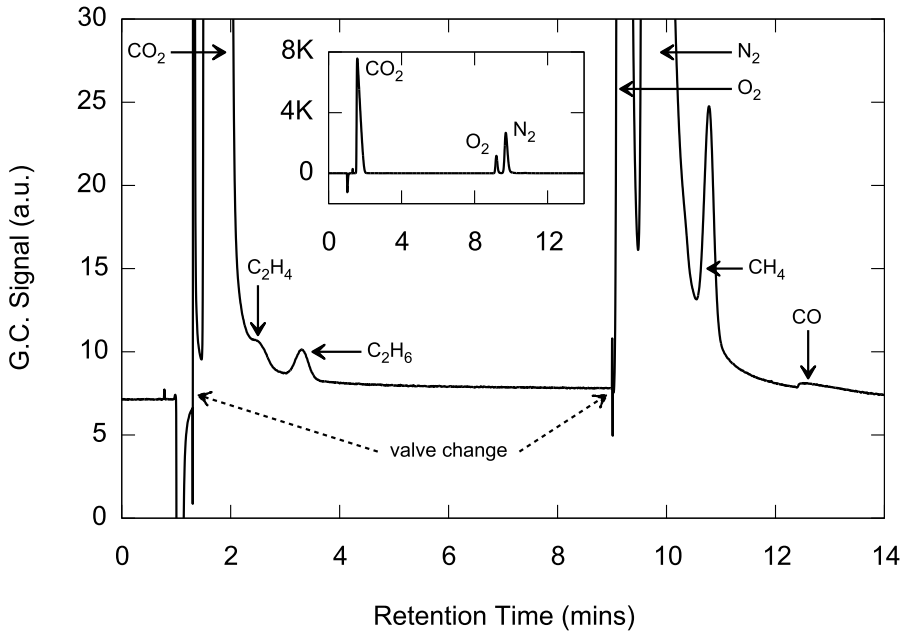

Figure S6. Representative example of a gas chromatogram for the products of CO_2 reduction at a nickel-gallium film. The example shows specifically results from electrolysis with Ni_5Ga_3 at −0.68 V vs. RHE in 0.1M Na_2CO_3 (aq) acidified to pH 6.8 with 1 atm CO_2 (g) where 150 C was passed. Given the poor separation between the C_2H_4 and CO_2 peaks at these concentrations, GC-MS rather than GC was used to quantify the F.E. for C_2H_4. Inset shows the full-scale chromatogram. Relative peak heights for O_2, N_2 and CO_2 are representative for both control experiments and bulk electrolyses.

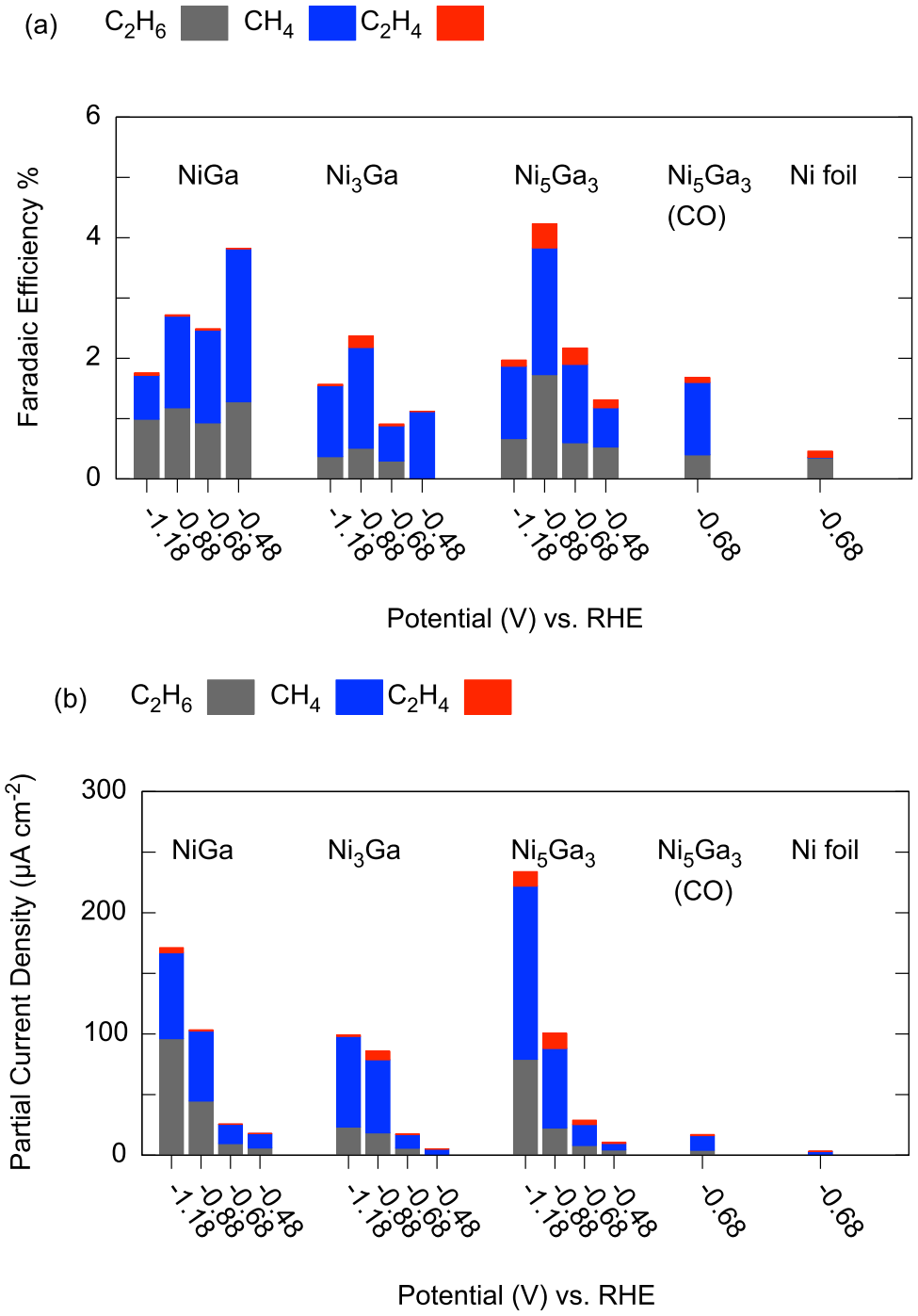

Figure S7. Histograms showing (a) Faradaic efficiency and (b) partial current density towards hydrocarbon products for the nickel-gallium films under CO_2 or under CO.

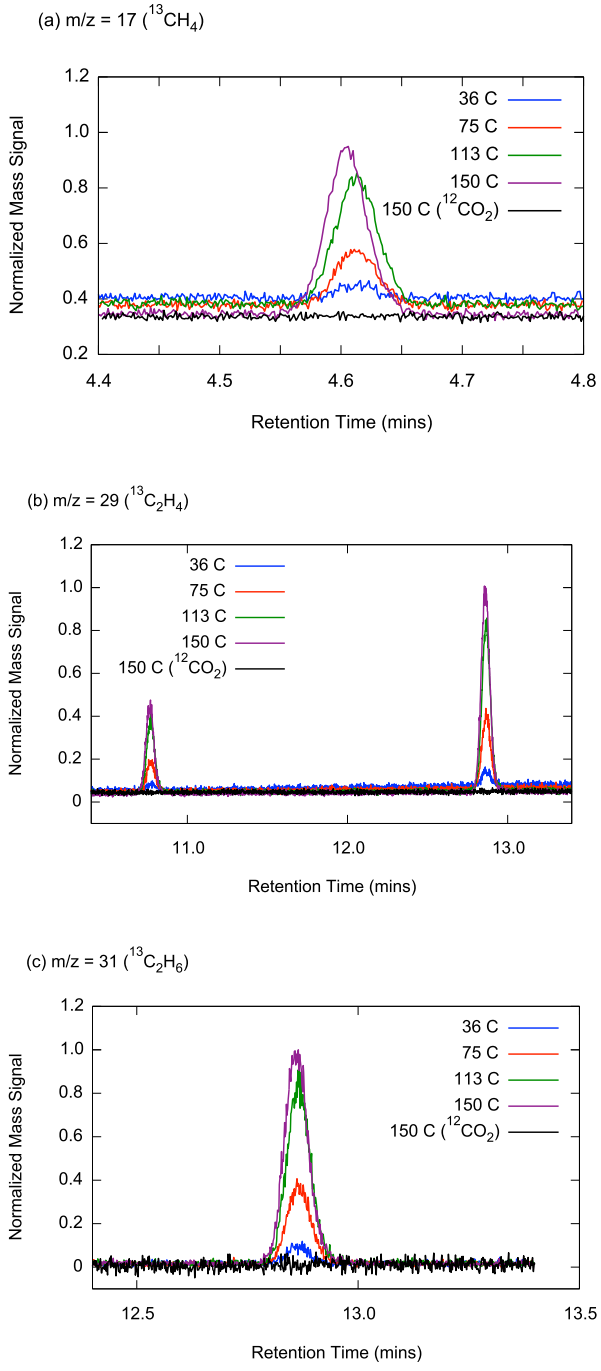

Figure S8. GC/MS data obtained during a $^{13}CO_2$ electroreduction. (a) m/z=17 corresponding to $^{13}CH_4$, (b) m/z=29: first peak corresponds to $^{13}C_2H_4$ and second peak to $^{13}C_2H_6$, (c) m/z=31 corresponding to $^{13}C_2H_6$. The number of Coulombs (C) of charge passed during the electrocatalysis when the products were analyzed is color-coded as indicated in the legends.

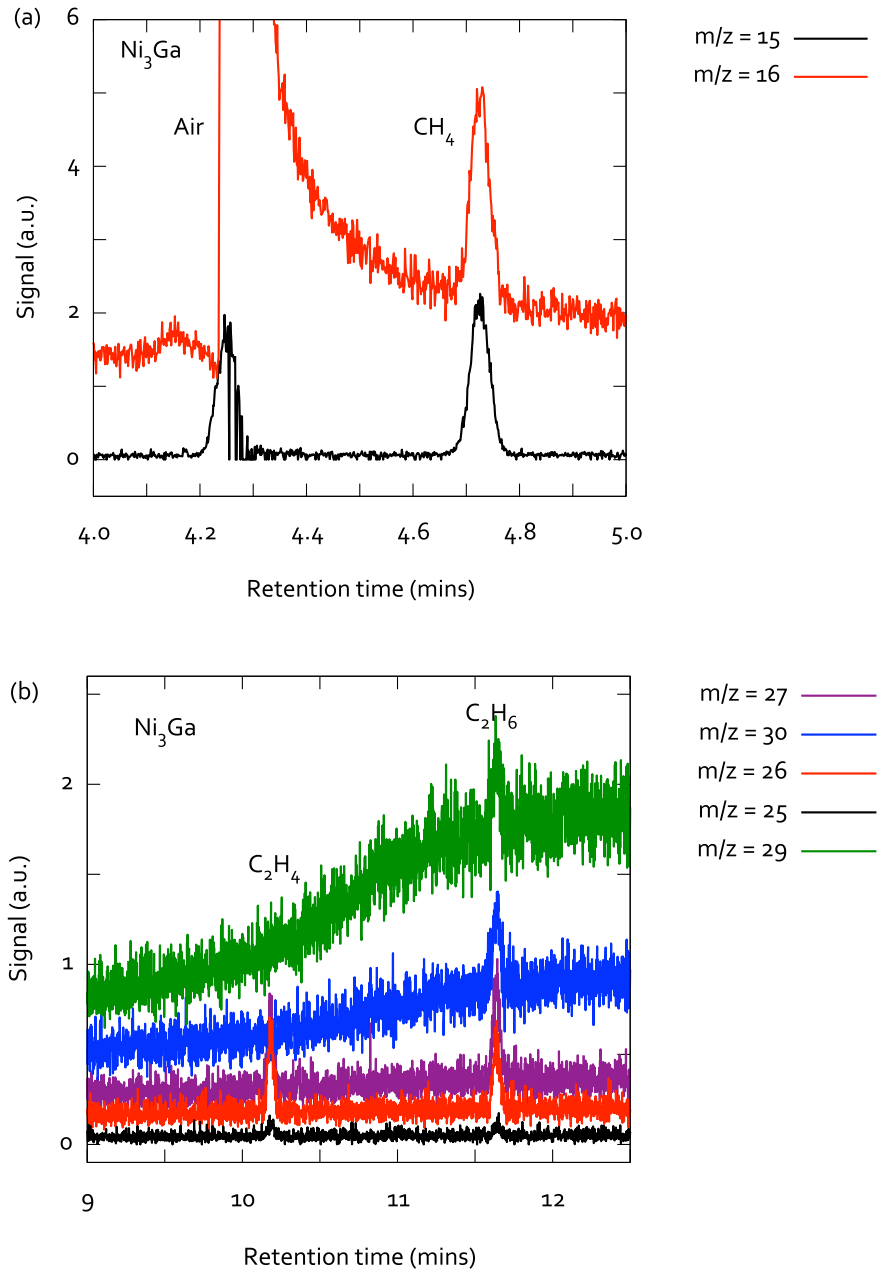

Figure S9. Example GC/MS chromatograms for each m/z fragment corresponding to CH_4, C_2H_4, and C_2H_6. (a) The signals corresponding to CH_4 at 4.7 min are m/z=16 (CH_4^+) and m/z= 15 (CH_3^+). Signals for m/z=14, 13, and 12 (CH_2^+, CH^+, and C^+) are roughly 5-6 times less intense than m/z=16 and 15 and therefore are not observed. The signal at 4.3 min corresponds to O_2 where m/z=16 (O^+) and N_2 where m/z = 15 (^{15}N-$^{14}N^+$). (b) The signals corresponding to C_2H_4 at 10.1 min are m/z=27 ($C_2H_3^+$), m/z= 26 ($C_2H_2^+$) and m/z=25 (C_2H^+). Because of the substantial N_2^+ background at m/z=28 ($C_2H_4^+$) is not observed. The signals corresponding to C_2H_6 at 11.8 min are m/z=30 ($C_2H_6^+$), m/z=29 ($C_2H_5^+$), m/z=27 ($C_2H_3^+$), m/z= 26 ($C_2H_2^+$) and m/z=25 (C_2H^+); again m/z=28 ($C_2H_4^+$) is not observed because of N_2^+ background.

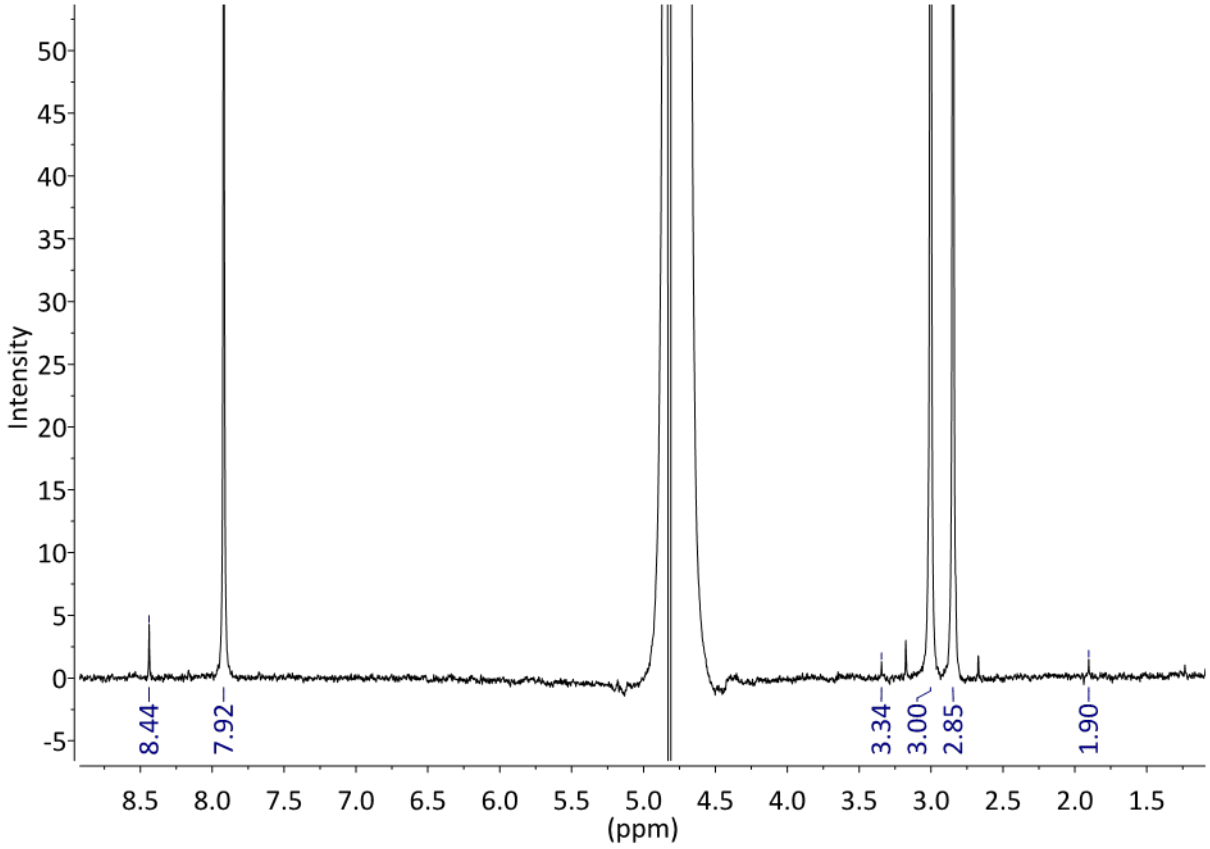

Figure S10. NMR spectra of the 0.1M Na_2CO_3 (aq) acidified to pH 6.8 with 1 atm CO_2 (g) after an electrolysis with NiGa at -1.2 V vs. RHE. The peak at 8.44 ppm corresponds to formate, the peaks at 7.92, 3.00, and 2.85 ppm correspond to the DMF internal standard at 65 μM, and the peak at 3.34 ppm corresponds to methanol. The peak at 1.90 ppm corresponds to acetate which is formed upon bubbling CO_2 into the solution. The large peak at 4.8 ppm corresponds to water.